

UNCLASSIFIED

Defense Technical Information Center  
Compilation Part Notice

ADP023644

TITLE: Plasma Research for Aerospace Propulsion

DISTRIBUTION: Approved for public release, distribution unlimited

This paper is part of the following report:

TITLE: Army Research Office and Air Force Office of Scientific Research  
Contractors' Meeting in Chemical Propulsion Held in Arlington, Virginia  
on June 12-14, 2006

To order the complete compilation report, use: ADA474195

The component part is provided here to allow users access to individually authored sections of proceedings, annals, symposia, etc. However, the component should be considered within the context of the overall compilation report and not as a stand-alone technical report.

The following component part numbers comprise the compilation report:

ADP023616 thru ADP023650

UNCLASSIFIED

# PLASMA RESEARCH FOR AEROSPACE PROPULSION

Principal Investigator: Biswa N. Ganguly

AFRL/PRPE  
WPAFB OH 45433

## SUMMARY/OVERVIEW:

Develop plasma devices for improved ignition, flame holding, and flow control. Also, generate microscopic non-equilibrium conditions to control macroscopic transport properties and kinetics of gas flows

## TECHNICAL DISCUSSION:

We report experimental investigations of the effects of DC electric fields on pre-mixed propane/air flames. The current study complements previous work<sup>1,2</sup> and extends recent results<sup>3</sup> which showed that dramatic modifications of the reaction zone of propane/air flames could be achieved with 3-6 kV applied voltages. Potential practical applications in a wide variety of combustors include providing for controlled flame holding and enhancement of reactant mixing, the latter possibly offering reductions in emissions of unwanted combustion products such as CO and carbon clusters (soot). More specialized applications to combustion in microgravity might also be possible.

Modest applied voltages are capable of driving the flame from laminar (stable, conical flame geometry) to a wrinkled laminar geometry (cellular; multiple laminar flamelets), with some evidence of the approach to turbulence regimes. The electric field acts directly on the highly localized, chemiionization-derived  $\text{H}_3\text{O}^+$ ,  $\text{HCO}^+$  and other positive ions in the flame reaction zone, significantly increasing their mass diffusivities and thereby modifying the Lewis numbers of the ionic species. The observed result is a diffusive-thermal instability, typical of flames with global Lewis numbers less than one; it is most likely caused by the production of H atom and OH radicals by the dissociative recombination of  $\text{H}_3\text{O}^+ + e \rightarrow \text{H}_2\text{O} + \text{H}$  or  $\text{H}_2 + \text{OH}$ , and  $\text{HCO}^+ + e \rightarrow \text{H} + \text{CO}$  near the burner head, which is the cathode surface for the polarity of the applied voltage. The increased differential diffusional velocity of the reaction zone positive ions strongly affects the bulk flame speed, and the thermo-diffusive instability results in the flame front collapsing toward the burner head and taking on a wrinkled laminar geometry. High-speed two-dimensional imaging of the flame response to a pulsed voltage showed that the characteristic time<sup>3</sup> required to complete the field-induced flame stretch is on the order of 5 ms, somewhat more rapid than that found in previous work<sup>4</sup>, but still indicative of the fluid mechanical nature of the flame response to the external field. Such images also show electric-field-induced unburned pocket formation which is a characteristic of turbulent combustion.

At higher continuous bias voltages (up to 6 kV), the flames are observed to make a further transition from cellular to highly turbulent flame fronts over a wide range of flow/bias voltage conditions. In much of the previous work<sup>1,2,4</sup>, the effects of DC electric fields on flames was described in terms of the body force known as the ionic wind, which has been shown to be capable of providing a maximum pressure difference across the flame<sup>3,5</sup> of only 0.0004 atm. This applied voltage-current induced pressure change is very small to cause the observed change in either the flame speed or the

flame heat release rate fluctuations through direct pressure effects. The DC-field-induced transition from laminar to highly turbulent combusting flows is quantified by direct high-speed imaging of the flame heat release rate fluctuations by measuring the chemiluminescence intensity using 200  $\mu$ sec gated ICCD as well as by wide band width spectral intensity measurements of flame radical species  $\text{CH}^*$ ,  $\text{C}_2^*$  and  $\text{OH}^*$  emissions. Fast Fourier Transforms (FFT) of the oscillating flame front emission signals were used to document the large differences between zero field (laminar flow) and DC-field driven turbulence conditions. Additionally, under DC applied voltage, the collapsed reaction zone is observed to undergo a transition from a low amplitude and low frequency oscillation typical of a laminar flame, to a large amplitude high frequency oscillation, similar to a thermo-acoustically perturbed flame<sup>6</sup>. Efforts to quantify these newly observed oscillatory modes of the flame front are presented.

The burner, used in this experiment, produces stable, laminar flow, conical reaction zones with a base diameter of 17 mm and height that varies with equivalence ratio and overall flow rate. Total flow rates varied between 12,000 – 30,000 sccm, which provides flow velocities on the axis of the burner from roughly twice propane's stoichiometric laminar flame speed (0.44 m/s) to well past the burner's blow off flow rate at zero applied voltage. Equivalence ratios used range from 0.8 to 1.4. DC fields are applied to the flames by connecting a 6 kV power supply across the grounded burner head, and positively biasing an electrode centered typically 40 mm above the grounded burner.

The magnitude of the current drawn, for a given applied voltage, with our anode configuration is nearly an order of magnitude higher than previously reported<sup>1, 2</sup> measurements for electrically biased pre-mixed hydrocarbon flames. Since the current is mobility limited, the larger current drawn at lower applied voltage will result in a significant increase of the positive ion flux in our experimental conditions, as compared to the previous measurements. If the dissociative recombination driven production of limiting light reactants is the source for the lowering of the Lewis number below a critical Lewis number, this could be one of the most important reason why it was possible to us achieve the level of thermo-diffusive instability that was not possible in previous measurements.

A transition from cellular flame structure, at lower pulsed applied voltage, to a flame instability caused by the larger pulsed applied voltage is presented in Figure 1, which shows an unburned pocket formation (images were acquired with 1 ms time separation), suggesting the onset of intense turbulence conditions. Chen et. al.<sup>7</sup> have published an extensive numerical study of the pocket formation, and among their findings they note that pocket formation, channel closing and pocket burnout all correspond to strongly curved flames.

The observations cited above, including the images of unburned pocket formation of Figure 1, point to the onset of significant levels of electric-field-induced turbulent combustion. Further improvements in the coupling of the electric field to the flame, and the use of a higher voltage DC power supply that permit larger electrical energy input to the flame would drive the flames toward increasingly turbulent conditions (i.e. increasingly smaller scale turbulence features) associated with the distributed reactions regime. At particular higher electric field/flow combinations (3-6 kV applied voltage), the electric pressure effect causes the flame front to undergo large amplitude, high frequency oscillations over large portions of the flame front surface. These conclusions are supported by the high speed, two-dimensional images of the flame front which includes  $\text{CH}^*$  emissions at 431 nm,  $\text{OH}^*$  emissions at 308 nm, and  $\text{C}_2$  emissions at 516 nm, as shown in Figures 2, 3, and 4 respectively. Those images show that OH and CH radicals are redistributed by the applied electric field in essentially the same way. However, the total integrated OH and CH emission intensities are independent of the applied field. Given that the electric field depresses the flame front toward the burner head, this behavior suggests that the effect of the thermo-diffusive instability is also to increase the combustion intensity.

The final data reported here are derived from measurements of the current and flame front optical signal oscillations. Figure 5 shows a series of fast Fourier transforms (FFTs) of broadband and spectrally

filtered flame front emissions, as well as the FFT of the oscillating current drawn from the external bias supply. Again, the experimental conditions are the same as those used for the imaging data shown in Figures 2, 3, and 4 (21 slm overall flow and equivalence ratio of 1.2) except that the bias used was only 4 kV.

The top left FFT of Figure 5 shows the very low amplitude, featureless power spectrum of the flame's broadband emissions under zero bias. It indicates stable laminar flow. With a 4 kV bias the flame front is driven into a large amplitude resonate-like oscillation with a fundamental frequency near 300 Hz and harmonics ranging up to 1.8 kHz. Essentially the same responses are seen again from broadband emissions and those corresponding to chemi-excited CH, C<sub>2</sub> and OH. Furthermore, the current passing through the flame also exhibits a power spectrum that is essentially identical to that of the flame front emissions. This is indicative that the voltage-current behavior is also dependent on the heat release rate modulation similar to the chemiluminescence intensity.

### References

1. Calcote, H.F. and Berman, C.H., in Fossil Fuels Combustion Symposium PD-Vol. 25, S.N. Singh, Ed., 25 (1989).
2. Bradley, D. and Nasser, S.H., *Combust. Flame* 55, 53 (1984).
3. Marcum, S.D. and Ganguly, B.N., *Combust. Flame* 143, 27 (2005).
4. Kono, M., Carleton, F.B., Jones, A.R. and Weinberg, F.J., *Combust. Flame* 78, 357 (1989).
5. Pedersen, T. and Brown, R.C., *Combust. Flame* 94, 433 (1993).
6. Nicuod, F and Poinso, T, *Combust. Flame* 142, 153 (2005).
7. Chen, J.H., Echehki, T., and Kollmann, W., *Combust. Flame* 116, 15 (1999)

### Figures:

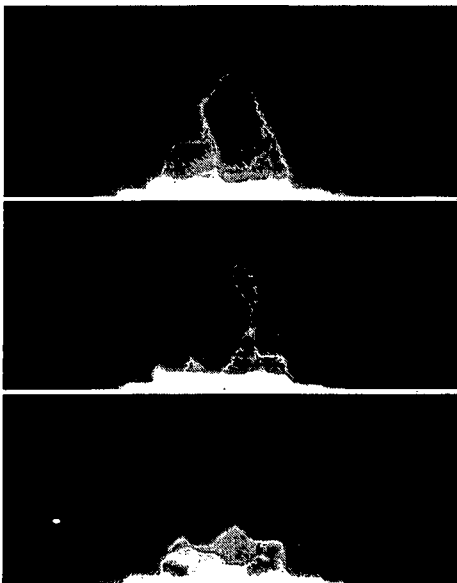


Figure 1. Images of unburned pocket formation.

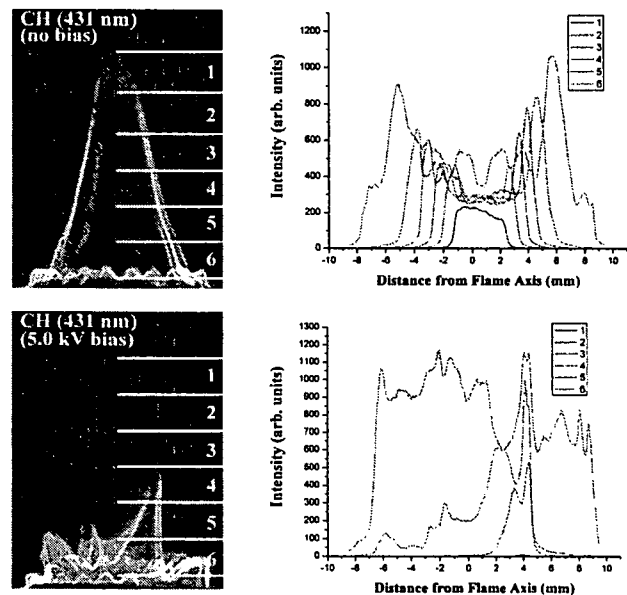


Figure 2. CH emission with and without applied voltage.

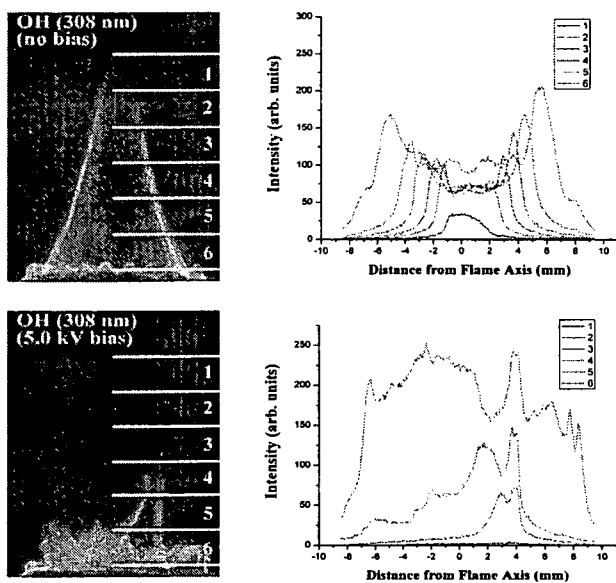


Figure 3. OH emission with and without applied voltage.

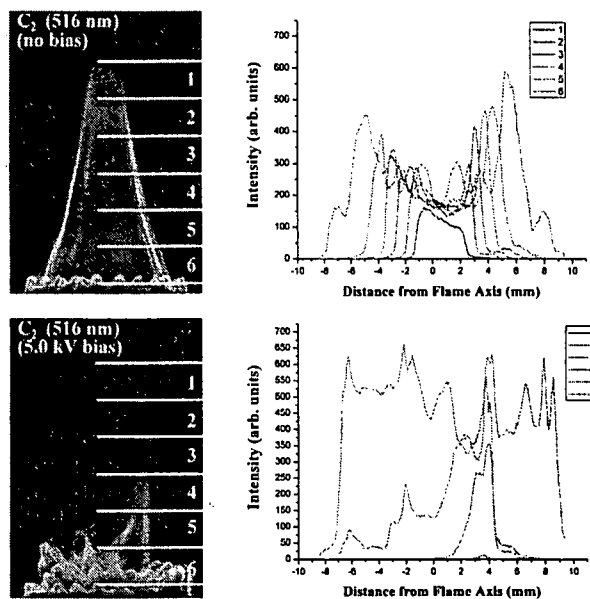


Figure 4. C<sub>2</sub> emission with and without applied voltage.

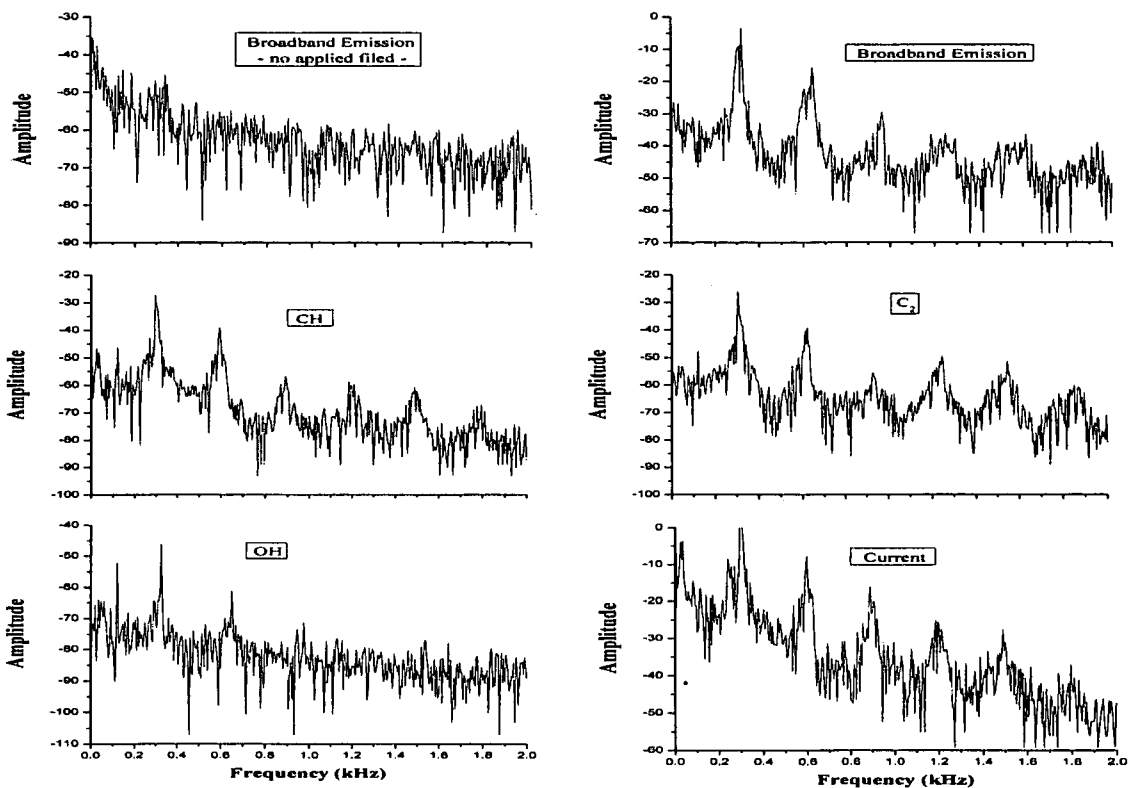


Figure 5. FFTs of broadband emission from unperturbed flame along with DC electric field induced perturbed flame and filtered CH, C<sub>2</sub> and OH chemiluminescence, and current fluctuations are shown.